The 2009 IEEE/RSJ International Conference on
Intelligent Robots and Systems
October 11-15, 2009 St. Louis, USA

Stochastic Static Analysis of Link Driven by Actuator Bundles

Takahiro Yoshimura, Mizuho Shibata, and Shinichi Hirai

Abstract— **This paper describes a stochastic static analysis of link angle driven by actuator bundles. We first demonstrate a movement of a link driven by actuator bundles in terms of high driving force. The variation of actuator parameters influences the movement of this mechanism. We confirm the link may shift and twist because of the variation of actuator parameters. We then introduce stochastic analysis to investigate the link angle considering the variation of actuator parameters. In the result, the variation of the link angle converges to zero when the number of actuator is large enough. In addition, we reinforce the result through dynamic simulation considering the variation of the parameters of actuators.**

I. Introduction

Human joints are composed by a lot of muscles. The joints are moved by cooperating with a lot of muscle fibers [1]. In the past decades, there have been several studies of mechanisms driven by a lot of actuators. Mizuuchi *et al*. have developed a robot including a flexible spine [2]. They have applied ninety-six tendon actuators, and proposed tendon length control, tendon tension control, and tendon spring control for the spine. Ikuta *et al*. have constructed an active endoscope using shape memory alloy (SMA) actuators [3]. Their endoscope can bend in three-dimensional direction using an electric resistance feedback for the SMAs. Mascaro *et al*. have presented a control method to drive an array of wet Shape Memory Alloy actuators [4]. Their architecture results in a vast DOF system that minimizes the number of valves and optimizes the use of them. They have made the 16 wet SMA actuators assembled in the 4x4 array as an application. Ueda *et al*. have studied a broadcast feedback approach to the distributed stochastic control of an actuator system consisting of many cellular units [5]. In that paper, stability conditions of the broadcast feedback system are obtained by using a stochastic Lyapunov function. We have proposed a link mechanism with compliance to construct a robotic hand [6]. The joint mechanism using a viscoelastic object and soft actuators instead of a cartilage and muscles of human arm is referred to as a *loosely coupled mechanism*. We also have constructed a control method of a 3D loosely coupled mechanism with length sensors [7]. In that paper, we realized the control of two projecting angles by the 3D prototype with multiple actuators. In that results, we have confirmed that the link mechanism applied by multiple actuators is useful as like human joint.

This paper describes a stochastic static analysis of link angle driven by actuator bundles. We first demonstrate a movement of a link driven by actuator bundles in terms of high driving force. The variation of actuator parameters influences the movement of this mechanism. We confirm the link may shift and twist because of the variation of actuator parameters. We then introduce stochastic analysis to investigate the link angle considering the variation of actuator parameters. In the result, the variation of the link angle converges to zero when the number of actuator is large enough. In addition, we reinforce the result through dynamic simulation considering the variation of the parameters of actuators.

II. Loosely Coupled Mechanism with Actuator Bundles

In this section, we demonstrate a movement of a link mechanism driven by actuator bundles. Figure 1 shows a loosely coupled mechanism using actuator bundles, which is driven in two-dimensional plane. In this mechanism, we apply shape-memory alloy (SMA) coils. In the figure, four antagonistic pairs of SMAs are arranged. All SMAs fixed on a common electrode; all SMAs shrink simultaneously during turning on electricity. An SMA has high driving force per unit weight in comparison with a DC motor and an engine [8]. In addition, multiple actuators yield high force. The way coincides that a muscle of human is composed by a lot of muscle fibers. Figure 2 shows driving forces of loosely coupled mechanism. The forces of the link using actuator bundles are larger than the one without bundles. Figure 3 shows an experimental result for angle control of the link using visual information. In this control, we apply

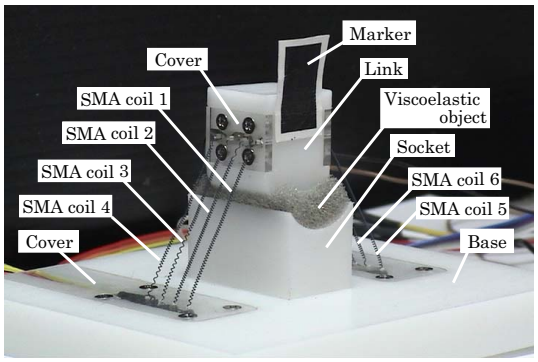

Fig. 1. Loosely coupled mechanism using SMA actuator bundles

T. Yoshimura is with Department of Robotics, Ritsumeikan Univ., 1-1-1 Noji-Higashi, Kusatsu, Shiga, 525-8577, Japan rr010031@se.ritsumei.ac.jp
M. Shibata is with Department of Robotics, Ritsumeikan Univ., 1-1-1 Noji-Higashi, Kusatsu, Shiga, 525-8577, Japan rr003983@se.ritsumei.ac.jp
S. hirai is with Department of Robotics, Ritsumeikan Univ., 1-1-1 Noji-Higashi, Kusatsu, Shiga, 525-8577, Japan hirai@se.ritsumei.ac.jp

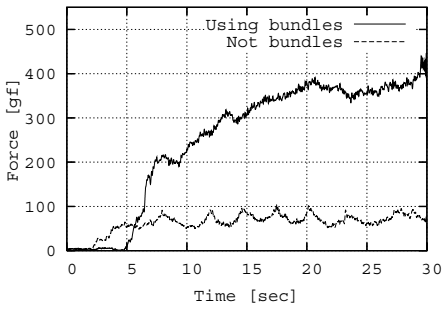

Fig. 2. Driving force by a loosely coupled mechanism

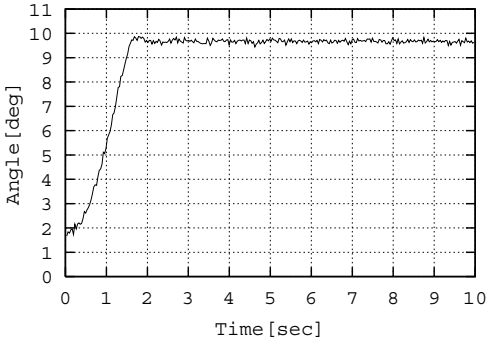

Fig. 3. Link angle of loosely coupled mechanism using actuator bundles

proportional control for the link angle. The desired angle is 10 degree. There is steady-state error, but the link angle converges.

We need to consider variation of actuator parameters because we deal with a lot of actuators. The influence of the variation of actuator parameters is not negligible. Figure 4 shows an experimental setup to measure the motion of the electrode only. In the figure, the link does not fixed on the electrode to confirm an influence of the variation of the actuator bundles clearly. We apply eight SMA coils as actuator bundles in this equipment. One end point of each SMA fixed on the electrode under gravity. The size and the mass of the electrode are $5{\times}20$ mm^2 and 1 g, respectively. We turn on electricity corresponding 4.5 V for all SMAs to shrink them. We observe the movement of the electrode during shrinkage of SMAs by a CMOS camera at 1000 Hz. Figure 5 shows successive images of the movement of the electrode in experiment. To control an angle of the link of Figure 1 in two-dimensional plane precisely, all SMAs shrink to all length after coming to rest. Unfortunately, there are variation of the actuator parameters so that the electrode shifts and twists as shown in Figure 5; the final lengths of the SMAs are not all same. In this paper, we investigate a link movement driven by actuator bundles considering the variation of the actuator parameters.

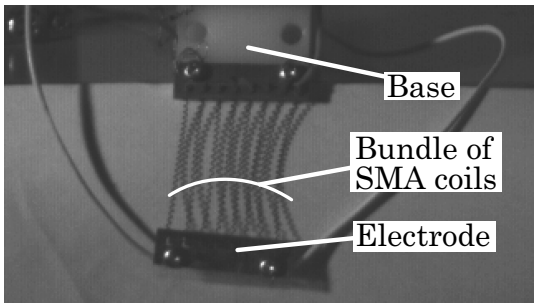

Fig. 4. Experimental setup for measuring motion of the electrode

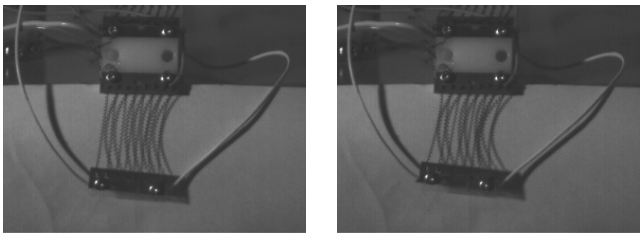

(a) 0.0 sec (b) 0.8 sec

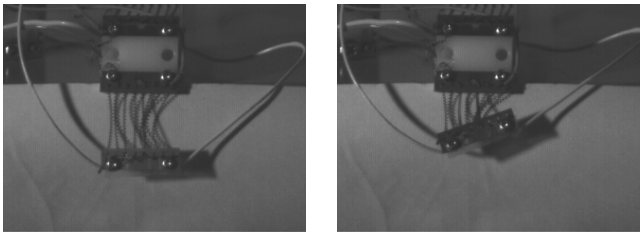

(a) 1.6 sec (b) 2.4 sec

Fig. 5. Motion of the electrode pulled by actuator bundles

III. Static Analysis Based on Probability

A. Angle Description

Figure 6 shows a model of an electrode driven by actuator bundles to analyze the link angle. We assume that the electrode is a link mechanism, and the link material is uniform. In this model, n springs fix on the link instead of actuator bundles under gravity. For simplicity, we assume that natural lengths of the springs are zero. One end of each spring is arranged on fixed end along x axis, and other end is arranged on the link. These fixed points are considered as free joints for rotation. Whole length of the link is $2L$. We assume that a distance between adjacent fixed points is $2L/n$. Let $\boldsymbol{x} = [x, y, \theta]^{\mathrm{T}}$ and m be the link position, angle, and mass, respectively. Deformation vector $\boldsymbol{d_i}$ of fixed point of the i-th spring on the link is descried as following equation:

$$\boldsymbol{d_i} = \begin{bmatrix} x + L_i(\cos\theta - 1) \\ y + L_i \sin\theta \end{bmatrix}, \tag{1}$$

where L_i is a distance between the center of the link and the fixed points on the link of the i-th spring. Distance L_i is calculated as follows:

$$L_i = \frac{L}{n-1}(n - 2i + 1). \tag{2}$$

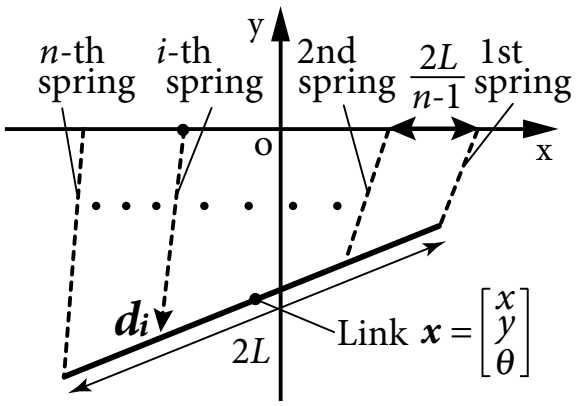

Fig. 6. Model of link mechanism for static analysis

Let K_i and g be stiffness of the i-th spring and gravitational acceleration. Whole energy U, calculated by summating energy of position and springs, of the system is described as:

$$U = mgy + \sum_{i=1}^{n} \left(\frac{1}{2} K_i |\boldsymbol{d_i}|^2 \right). \tag{3}$$

When the link comes to rest at equilibrium position, energy U reaches local minimal value; $\partial U / \partial \boldsymbol{x} = \boldsymbol{0}$ is satisfied. To derive the link angle at equilibrium position, we calculate $|\boldsymbol{d_i}|^2$ as:

$$\begin{aligned} |\boldsymbol{d_i}|^2 &= x^2 + 2xL_i(\cos\theta - 1) + y^2 + 2yL_i \sin\theta \\ &\quad -2L_i^2 \cos\theta + 2L_i^2. \end{aligned} \tag{4}$$

Partial differential value of energy U for x is described as:

$$\begin{aligned} \frac{\partial U}{\partial x} &= \sum_{i=1}^{n} \left\{ \frac{\partial}{\partial x} \left(\frac{1}{2} K_i |\boldsymbol{d_i}|^2 \right) \right\} \\ &= \sum_{i=1}^{n} K_i x + \sum_{i=1}^{n} K_i L_i (\cos\theta - 1) = 0. \end{aligned} \tag{5}$$

Hence, x is calculated as:

$$x = \frac{(1 - \cos\theta)\beta}{\alpha}, \tag{6}$$

where α, β are as follows:

$$\alpha = \sum_{i=1}^{n} K_i, \tag{7}$$

$$\beta = \sum_{i=1}^{n} K_i L_i. \tag{8}$$

In the same way, y is described as:

$$\begin{aligned} \frac{\partial U}{\partial y} &= mg + \sum_{i=1}^{n} \left\{ \frac{\partial}{\partial y} \left(\frac{1}{2} K_i |\boldsymbol{d_i}|^2 \right) \right\} \\ &= mg + \sum_{i=1}^{n} K_i y + \sum_{i=1}^{n} K_i L_i \sin\theta = 0. \end{aligned} \tag{9}$$

Hence, y is calculated as:

$$y = \frac{-mg - \beta \sin\theta}{\alpha}. \tag{10}$$

In the same way, θ is described as:

$$\begin{aligned} \frac{\partial U}{\partial \theta} &= \sum_{i=1}^{n} \left\{ \frac{\partial}{\partial \theta} \left(\frac{1}{2} K_i |\boldsymbol{d_i}|^2 \right) \right\} \\ &= -\sum_{i=1}^{n} K_i L_i x \sin\theta + \sum_{i=1}^{n} K_i L_i y \cos\theta \\ &\quad + \sum_{i=1}^{n} K_i L_i^2 \sin\theta \\ &= -\beta x \sin\theta + \beta y \cos\theta + \gamma \sin\theta = 0, \end{aligned} \tag{11}$$

where γ is as follows:

$$\gamma = \sum_{i=1}^{n} K_i L_i^2. \tag{12}$$

Using Eqs. 6, 10, and 11, we have $\tan\theta$ as follows:

$$\tan\theta = \frac{mg\beta}{\alpha\gamma - \beta^2}. \tag{13}$$

Using Eq. 2, the tangent of the link angle is substituted as:

$$\begin{aligned} \tan\theta &= \frac{mg\beta}{\alpha\gamma - \beta^2} \\ &= \frac{mg \sum_{i=1}^{n} K_i \frac{n-2i+1}{n-1} L}{4 \left(\frac{L}{n-1} \right)^2 \sum_{i=1}^{n-1} \sum_{j=i+1}^{n} (i-j)^2 K_i K_j} \\ &= \frac{mg(n-1)}{4L} \frac{\sum_{i=1}^{n} (n-2i+1) K_i}{\sum_{i=1}^{n-1} \sum_{j=i+1}^{n} (i-j)^2 K_i K_j} \\ &= \frac{mg(n-1)}{4L} \frac{F}{G}, \end{aligned} \tag{14}$$

where F and G are:

$$F = \sum_{i=1}^{n} (n - 2i + 1) K_i, \tag{15}$$

$$G = \sum_{i=1}^{n-1} \sum_{j=i+1}^{n} (i-j)^2 K_i K_j. \tag{16}$$

B. Probability Distribution of Link angle

In this section, we investigate a relationship between the probability distribution of a link driven by actuator bundles and the number of the actuators, considering the variation of actuators. Let μ and σ^2 be the average and the variance of the stiffness K_i of the spring. To get the distribution of the link angle, we need to calculate the probability distribution of Eq. 14. However, it is difficult to calculate directly the distribution of Eq. 14 using the probabilistic distribution of K_i. We evaluate the distribution of Eq. 14 based on the average and the variance of F and G. We first calculate the

expectation value of K_i^2 in advance:

$$\begin{aligned}\mathbf{V}(K_i) &= \mathbf{E}\left((\mathbf{E}(K_i)-K_i)^2\right)\\ &= \mathbf{E}\left((\mu-K_i)^2\right)\\ &= \mu^2-2\mu\mathbf{E}(K_i)+\mathbf{E}\left(K_i^2\right)\\ &= \mu^2-2\mu^2+\mathbf{E}\left(K_i^2\right)=\sigma^2. \end{aligned} \quad (17)$$

Hence, the expectation value $E({K_i}^2)$ is calculated as:

$$\mathbf{E}\left(K_i^2\right) = \mu^2+\sigma^2. \quad (18)$$

We derive the average and the variance of F. Using Eq. 15, the average $\mathbf{E}(F)$ is calculated as:

$$\begin{aligned}\mathbf{E}(F) &= \mathbf{E}\left(\sum_{i=1}^{n}(n-2i+1)K_i\right)\\ &= \mu\left\{\sum_{i=1}^{n}(n+1)-2\sum_{i=1}^{n}i\right\}\\ &= \mu\left\{n(n+1)-n(n+1)\right\}=0. \end{aligned} \quad (19)$$

Using Eq. 18, the variance $\mathbf{V}(F)$ is calculated as:

$$\begin{aligned}\mathbf{V}(F) &= \mathbf{E}\left((\mathbf{E}(F)-F)^2\right)\\ &= \mathbf{E}\left(\left(\sum_{i=1}^{n}(n-2i+1)K_i\right)^2\right)\\ &= \frac{n}{3}(n+1)(n-1)\sigma^2. \end{aligned} \quad (20)$$

We derive the average and the variance of G. Using Eq. 16, the average $\mathbf{E}(G)$ is calculated as:

$$\begin{aligned}\mathbf{E}(G) &= \mathbf{E}\left(\sum_{i=1}^{n-1}\sum_{j=i+1}^{n}(i-j)^2K_iK_j\right)\\ &= \sum_{i=1}^{n-1}\sum_{j=i+1}^{n}(i-j)^2\mathbf{E}(K_iK_j)\\ &= \mu^2\sum_{i=1}^{n-1}\sum_{j=i+1}^{n}\left(j^2-2ij+i^2\right)\\ &= \frac{\mu^2}{12}n^2(n-1)(n+1). \end{aligned} \quad (21)$$

The variance $\mathbf{V}(G)$ is calculated as:

$$\begin{aligned}\mathbf{V}(G) &= \mathbf{E}\left((\mathbf{E}(G)-G)^2\right)\\ &= \mathbf{E}\left(\mathbf{E}(G)^2-2G\mathbf{E}(G)+G^2\right)\\ &= \mathbf{E}(G)^2-2\mathbf{E}(G)\cdot\mathbf{E}(G)+\mathbf{E}\left(G^2\right)\\ &= -\mathbf{E}(G)^2+\mathbf{E}\left(G^2\right). \end{aligned} \quad (22)$$

Here, the expectation value $\mathbf{E}\left(G^2\right)$ is calculated as:

$$\begin{aligned}\mathbf{E}\left(G^2\right) = \frac{\mu^2(\mu^2+\sigma^2)}{60}n^2(2n^5-4n^4-5n^3\\ +10n^2+3n-6). \end{aligned} \quad (23)$$

Hence, the variance $\mathbf{V}(G)$ in Eq. 22 is substituted as follows:

$$\begin{aligned}\mathbf{V}(G) &= -\mathbf{E}(G)^2+\mathbf{E}\left(G^2\right)\\ &= \frac{n\mu^2\sigma^2+\sigma^4}{60}n^2\left(2n^2-3\right)(n+1)(n-1). \end{aligned} \quad (24)$$

We assume that the probability distributions of F and G are normal. In normal probability distribution, the values within $\mu\pm3\sigma$ account for 99.7 % of the total [9]. Based on this theory, we investigate the practical maximum and minimum link angle within $\mu\pm3\sigma$. The maximum value H_+ of the link angle within $\mu\pm3\sigma$ is calculated as:

$$H_+ = \frac{3\sqrt{\mathbf{V}(F)}}{\mathbf{E}(G)-3\sqrt{\mathbf{V}(G)}}\frac{mg}{4L}(n-1) \quad (25)$$

Also, the maximum value H_+ of the link angle within $\mu\pm3\sigma$ is calculated as:

$$H_- = \frac{-3\sqrt{\mathbf{V}(F)}}{\mathbf{E}(G)-3\sqrt{\mathbf{V}(G)}}\frac{mg}{4L}(n-1) \quad (26)$$

Hence, if the number of the actuators is large enough, the following equations are satisfied:

$$\lim_{n\to\infty}H_+=0, \quad \lim_{n\to\infty}H_-=0. \quad (27)$$

Therefore, the expectation value of the link angle considering variation of the actuator converges to zero based on the squeeze theorem. Figure 7 shows the numerical example to confirm the validity in Eq. 27 based on Eqs. 25 and 26. In evaluation, we use parameters that the mass m, the link angle L, and the gravitational acceleration g are 1 g, 20 mm, 9.8 m/s^2, respectively. We assume that the average μ of the spring stiffness is 5 g/mm. In Figure 7-(a), we set the standard deviation σ to 1.5 g/mm; the stiffness is between 0.5 and 9.5 g/mm in normal probability distribution. In Figure 7-(b), we set the standard deviation σ to 0.1 g/mm; the stiffness is between 4.7 and 5.3 g/mm in normal probability distribution. From figures, we confirm that the maximum of the link angle decrease monotonically and converge to zero degree. In addition, the minimum of the link angle increase monotonically and converge to zero degree. In this paper, we do not calculate directly the distribution of Eq. 14. However, the range of the real distribution of Eq. 14 is small in comparison with the range based on Eqs. 25 and 26. Hence, the link angle converges to zero if we use a lot of actuators enough.

IV. Investigation through simulation

The results in previous section indicate that the angle control by the flexible joint we propose is useful. The link converges to desired value without twisting in angle control if we use a lot of actuators enough. In this section, we investigate the validity of the results through simulation. In this simulation, we investigate dynamically the link angle considering variation of actuator parameters. We apply an SMA as an actuator, which shrinks by turning on electricity. We apply the Madill's model to simulate the dynamics of SMAs [10]. Their model considers minor loops of SMAs; the amount of the martensite can be calculated even if plus and minus of current input switch during deformation of an SMA. We assume that the link moves two-dimensional

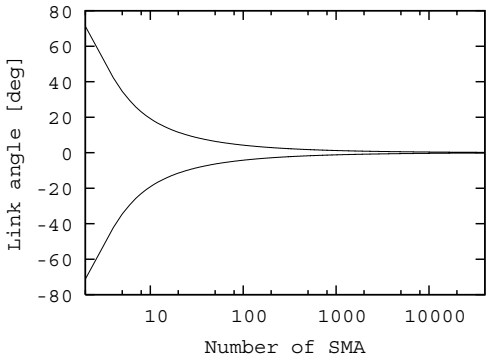

(a) $\sigma = 1.5$

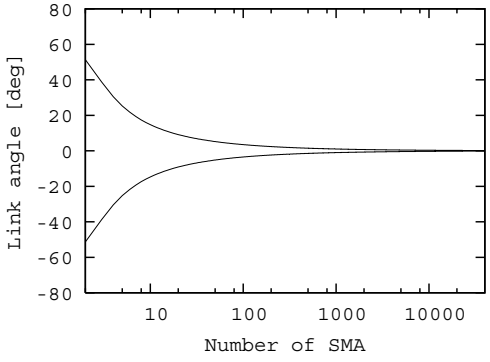

(b) $\sigma = 0.1$

Fig. 7. Maximum and minimum link angle

TABLE I
PARAMETERS FOR SIMULATION

Symbols	Value
ρ	6.5 $\times 10^{-3}$ g/mm^3
C_p	0.5 J/g deg C
V	2.96 mm^3
R_0	6.0 Ω
h	7.0 $\times 10^{-4}$ W/mm^2 deg C
A	59.2 mm^2
T_∞	25 deg C
k_m^C	0.62 1/deg C
k_m^H	0.62 1/deg C
M_s	42.0 deg C
M_f	32.0 deg C
A_s	60.0 deg C
A_f	70.0 deg C
R_{ma0}	1.0
R_{mb0}	0.0

plane. We set initial position of the link to $(x, y, \theta) = (0, -10, 0)$. The length and the mass of the link are 20 mm and 1 g, respectively. The variation of actuator parameters is represented as the variation of the stiffness. The variation of the stiffness is determined by uniform random numbers based on Mersenne Twister [11]. The stiffness after martensitic transformation $k_{\max}$ is set to the value between 5.5 g/mm and 4.5 g/mm, In addition, the stiffness before martensitic transformation $k_{\min}$ is set to the value between 0.5 g/mm and 1.5 g/mm. Table I shows another parameters of SMAs. The symbols are pursuant in literature [10].

We simulate the link movement increasing the number of SMAs. We check the movement between two and thirty SMAs. We simulate 30000 times at each number of SMAs. In this simulation, we observe the angle after the link comes to rest. Figure 8 shows the cumulative distribution function (CDF) and the probability density function (PDF). The value of the cumulative distribution function is the derivation of the probability density function. From Figure 8-(a) and (b), we confirm that the link angle is easy to converge to zero if the number of SMAs increases. Figures 8-(c) and (d) show the PDF with 2 and 30 SMAs. We confirm that the value in Figures 8-(d) is one thirtieth smaller than the value Figures 8-(c) from figures. In addition, the dash lines in Figures 8-(c) and (d) depict approximate lines in case that the lines are normal distribution functions. The shape of respective graph is similar to the respective normal distribution function. These simulation results reinforce the results in Section III. Figures 9 and 10 show the average and the standard deviation of the link, respectively. In Figure 9, the average converges to zero as the number of SMAs increase. In Figure 10, the standard deviation decrease as the number of SMAs increase. These simulation results also reinforce the results in Section III.

V. CONCLUSION

This paper described a stochastic static analysis of link angle driven by actuator bundles. We first demonstrated a movement of a link driven by actuator bundles in terms of high driving force. The variation of actuator parameters influenced the movement of this mechanism. We confirmed the link may shift and twist because of the variation of actuator parameters. We then introduced stochastic analysis to investigate the link angle considering the variation of actuator parameters. In the result, the variation of the link angle converged to zero when the number of actuator was large enough. In addition, we reinforced the result through dynamic simulation considering the variation of the parameters of actuators.

ACKNOWLEDGMENT

This research was partly supported by a fund for Grants-in-Aid for Scientific Research in Japan Society for the Promotion of Science (No. 19800054).

REFERENCES

[1] P.V. Komi, and C. Nicol: "Stretch-Shortening Cycle Fatigue", Biomechanics and biology of movement, pp.385-408, Human Kinetics, 2000.
[2] I. Mizuuchi, S. Yoshida, M. Inaba, and H. Inoue: "The development and control of a flexible-spine for a human-form robot", Advanced Robotics Vol.17, No.2, pp179-196, 2003.
[3] K. Ikuta, M. Tsukamoto, and S. Hirose: "Shape Memory Alloy Servo Actuator System with Electric Resistance Feedback and Application for Active Endoscope", Proc. of IEEE Int. Conf. on Robotics and Automation, pp.427-430, 1998.
[4] S. Mascaro and L. Flemming: "Control of Scalable Wet SMA Actuator Arrays", Proc. of IEEE Int. Conf. on Robotics and Automation, pp.1338-1343, 2005.

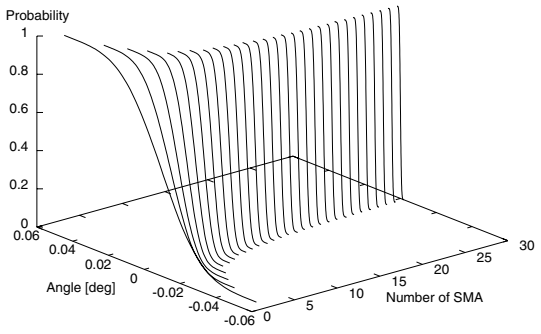

(a) CDF

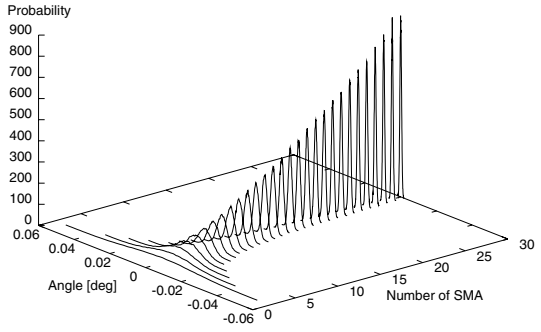

(b) PDF

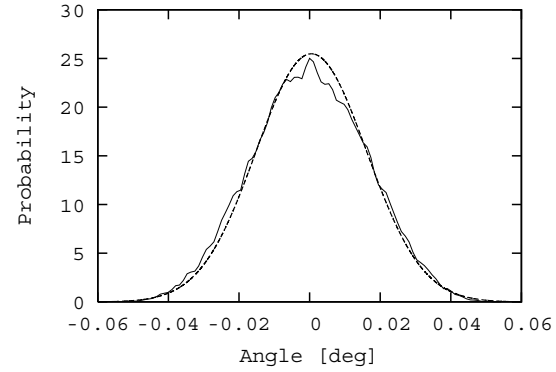

(c) PDF with 2 SMA coils

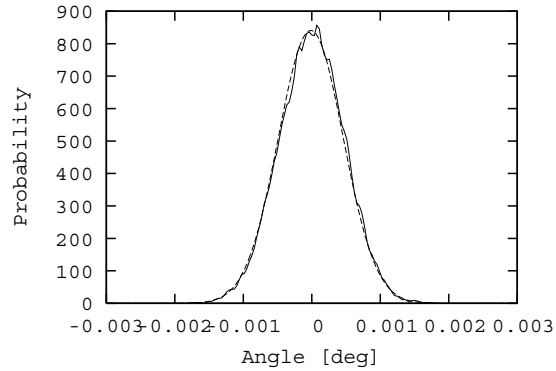

(d) PDF with 30 SMA coils

Fig. 8. Distribution of simulated link angle

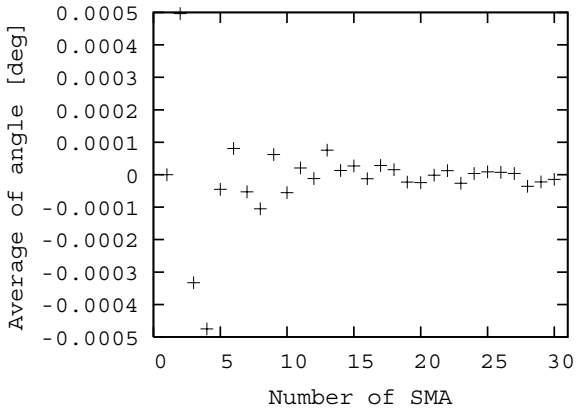

Fig. 9. Average of link angle

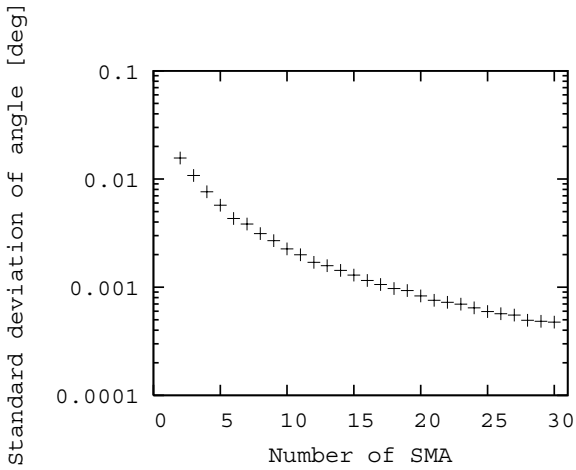

Fig. 10. Standard deviation of link angle

[5] J. Ueda, L. Odhner, and H. H. Asada: "Broadcast Feedback of Stochastic Cellular Actuators Inspired by Biological Muscle Control", The Int. Journal of Robotics Research, Vol. 26, pp. 1251-1265, 2007.

[6] M. Shibata, T. Yoshimura and S. Hirai: "Loosely Coupled Joint Driven by SMA Coil Actuators", Proc. of IEEE Int. Conf. on Robotics and Automation, pp.4460-4465, 2007.

[7] M. Shibata, T. Yoshimura, and S. Hirai: "Angle Control of Loosely Coupled Mechanism in 3D Space Using Length Sensors", Proc. IEEE/RSJ Int. Conf. on Intelligent Robots and Systems, pp.1178-1183, 2007.

[8] K. Ikuta, M. Tsukamoto, and S. Hirose: "Mathematical Model and Experimental Verification of Shape Memory Alloy for Designing Micro Actuator", Proc. of IEEE Micro Electro Mechanical Systems, pp.103-108, 1991.

[9] J. Devore and R. Peck: "Statistics : the exploration and analysis of data", Thomson Brooks/Cole, 2005.

[10] D. R. Madill and D. Wang: "Modeling and L2-Stability of a Shape Memory Alloy Position Control System", IEEE Transactions on control systems technology, Vol.6, No.4, pp.473-481, 1998.

[11] M. Saito, M. Matsumoto: "SIMD-oriented Fast Mersenne Twister: a 128-bit Pseudorandom Number Generator", Monte Carlo and Quasi-Monte Carlo Methods 2006, pp.607-622, 2008.